#### Journal of Nuclear Materials 510 (2018) 396-413

Contents lists available at ScienceDirect

# Journal of Nuclear Materials

journal homepage: www.elsevier.com/locate/jnucmat

## Radiation tolerance of commercial and advanced alloys for core internals: a comprehensive microstructural characterization

Miao Song<sup>a,\*</sup>, Calvin R. Lear<sup>a</sup>, Chad M. Parish<sup>b</sup>, Mi Wang<sup>a</sup>, Gary S. Was<sup>a</sup>

<sup>a</sup> Nuclear Engineering and Radiological Sciences, University of Michigan, Ann Arbor, MI, 48109, USA <sup>b</sup> Materials Science and Technology Division, Oak Ridge National Laboratory, Oak Ridge, TN, 37831, USA

### ARTICLE INFO

Article history: Received 14 May 2018 Received in revised form 14 August 2018 Accepted 16 August 2018 Available online 17 August 2018

Keywords: Radiation damage Structure material Microstructure Nickel-base alloy Precipitate

## ABSTRACT

Thirteen austenitic stainless steels, nickel-base alloys, and ferritic alloys were irradiated using 2 MeV protons at 360 °C to a damage level of 2.5 displacements per atom (dpa). Comprehensive microstructural characterization was performed for irradiation-induced features, including dislocation loops, voids, precipitates, and radiation induced segregation (RIS). Dislocation loops formed in all alloys except 14YWT, while voids were observed in alloys 316 L, 310, C22, and 14YWT. Irradiation-induced formation of  $\gamma'$  precipitates was observed in alloys 316 L, 310, 800, and 690; the irradiation-enhanced, long-range ordered Ni<sub>2</sub>Cr phase (Pt<sub>2</sub>Mo-type) was observed in alloys 690, C22, 625, 625Plus, 625DA, and 725; and Gphase was observed in alloy T92. No irradiation-induced precipitates were observed in alloys X750, 718 or 14YWT. Precipitation of the  $\gamma'$  phase can be understood through segregation and clustering of Si, Al, and Ti. Overall, austenitic stainless steels are generally susceptible to irradiation damage in the form of loops, voids, precipitates, and RIS. Ni-base alloys have this same type of dislocation loops and RIS behaviors but are more resistant to void swelling. Ferritic alloys showed better resistance to loop formation, void swelling and irradiation-induced precipitation. From the degree of irradiation-induced microstructural change, alloy T92 was identified as the most radiation resistant among these alloys.

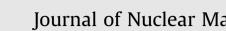
© 2018 Elsevier B.V. All rights reserved.

### 1. Introduction

The life extension of current operating reactors and the design of next generation nuclear reactors call for advanced materials that can maintain structural integrity in harsh radiation environments [1,2]. These materials must demonstrate better tolerance to high neutron flux (beyond 100 dpa), where void swelling, embrittlement, loss of fracture toughness, and irradiation-assisted stress corrosion cracking (IASCC) become the dominant degradation modes [3]. Among these concerns, IASCC is considered to be the primary degradation mode for light water reactor (LWR) core internals because of its widespread occurrence in load-bearing structural components at a relatively low damage (0.7 dpa to a few dpa [4]). Austenitic stainless steels (SSs) 304 and 316 as well as, nickel-base alloys 600, X750, and 718 have all shown susceptibility to IASCC [5], when used as fuel cladding, control rod blades, and various bolts and springs in pressurized water reactors (PWRs) or boiling water reactors (BWRs). This IASCC degradation may become more pronounced as reactors age during extended operation, making understanding and mitigation of IASCC essential.

Although advances have been made in understanding IASCC phenomenon, irradiation-induced microstructure, microchemistry of materials, and environmental conditions (i.e., temperature, water chemistry, radiolysis, and stress) are known to affect IASCC susceptibility, obscuring the underlying mechanism [5–9]. Among these factors, irradiation-induced microstructure and microchemistry of materials are critical to understanding IASCC behavior, because these internal features determine the response of materials under external factors (corrosion and stress). Therefore, an understanding of IASCC must start with microstructural evolution under irradiation.

Irradiation-induced loops, cavities, and precipitates can serve as barriers to dislocation motion, promote irradiation hardening and embrittlement, and adversely impact IASCC susceptibility. Radiation induced segregation (RIS) at grain boundaries (GBs) may further contribute to IASCC. Cr depletion at GBs may lead to passivation failure, and increase the susceptibility to IASCC. Segregated B and S at GBs potentially enhance the susceptibility of







IASCC through transmutation, where the former leads to the production of He [9]. These species could potentially reduce the cohesive strength of GBs or interact with water to advance cracks or accelerate intergranular corrosion [10].

Under LWR conditions, neutron irradiation of 300 series austenitic SS induces Frank loops or faulted loops ( $b = \frac{1}{3} < 111 >$ ), cavities, precipitates, and chemical segregation [11]. The dislocation network of cold-worked 316SS recovers after irradiation to 4 dpa [12]. Frank loops typically dominate the microstructure of irradiated SSs, the number density of which usually saturates after a few dpa [4]. Nano-sized cavities may form in cold-worked 316 L SS as early as 1 dpa, with a number density comparable to or higher than dislocation loop and with typical sizes of 3 nm [12,13] that may increase in the presence of gamma heating at high dose [14].  $\gamma'$  precipitates were frequently observed starting at 4 dpa [12,14], forming from the segregation and clustering of Ni and Si at network dislocations or loops. Irradiation-induced  $\alpha$ ferrite particles were reported in 304 S S after 5.5 dpa [15]. As for RIS at GBs, depletion of Cr occurs concurrently with Fe depletion and Ni enrichment [4]. While Mn, Ti, and Mo tend to deplete [9,14], both Si and P are enriched to several times their bulk contents [4].

Irradiated microstructures of nickel-base alloys are less understood in LWR relevant conditions than austenitic SSs. In nickel-base alloys, the same kind of faulted loops are frequently observed in alloys 718 [16], X750, and direct aged 625 (625DA) [17] irradiated to different doses. Nano-voids were observed in alloy X750 after 0.35 dpa [17], and in alloy 718 after 20 dpa [16]. However, helium bubbles (within the matrix, along GBs, and along matrix-particle interfaces) were the dominant feature in alloy X750 after a service life of ~55 dpa in a CANDU (CANada Deuterium Uranium) reactor [18]. Irradiation-induced Pt<sub>2</sub>Motype (long-range ordered) precipitates were observed in 625DA after 0.35 dpa [17]. Further, pre-existing  $\gamma'$  and  $\gamma''$  phases were frequently changed by irradiation. Stacking faults formed in  $\gamma'$ precipitates in alloy X750, while  $\gamma''$  precipitates tended to dissolve in alloy 625DA after 0.35 dpa [17]. The  $\gamma''$  phase was unchanged in alloy 718 after 0.14 dpa [19] but disappeared by 3.5 dpa in a second heat [16], indicating a pseudo-threshold dpa for dissolution or disordering. This disappearance was accompanied by the refinement of  $\gamma'$  precipitates [16]. RIS in nickel-base alloys follows a similar behavior to SSs, for example in alloy 718 [16]. However, in alloy X750, the transmutation of boron to helium at GB was responsible for IASCC [17].

Although limited data are available for ferritic and ferriticmartensitic (F/M) alloys under LWR conditions, the microstructural response of these alloys can be gleaned from works done in faster reactors. In F/M steels, <100> and  $\frac{1}{2}<111>$  type loops are most common [20]. Voids were observed in both Fe-9Cr and Fe-12Cr alloys irradiated to 35 dpa in a fast reactor at 420 °C [21], as well as in EP-450 steel irradiated at 380 °C to 56 dpa [22]. Nanocavities were also observed in T91 after 4.4 dpa at 469 °C [23]. Both chi-phase and  $\alpha'$  phase were observed in 12Cr alloys after 35dpa [21], with  $\alpha'$  precipitates also observed in irradiated EP-450 [22]. This irradiation-induced phase separation (i.e., formation of  $\alpha'$ ) is consistent with a later small angle neutron scattering experiment [24]. G-phase precipitation was reported at relative high doses in HT9 (155 dpa, 443 °C) [25] and in T91 (184dpa, 413 °C) [26]. However, a recent study also shows G-phase formation in T91 at only ~18 dpa (376-415 °C) [27]. Due to the low solubility of Cu in Fe, Cu-rich precipitates were frequently observed in irradiated F/M steels [27]. RIS in alloys Fe-9Cr, T91, NF616, and 14YWT below 600 °C typically enriches Cr, Ni, and Si, while depleting Fe [28]. A crossover temperature was observed where Cr enrichment changes to depletion, while Fe depletion reverts to enrichment between 600 °C and 700 °C [28]. Results for RIS in T91 irradiated in BOR60 concurs with these enrichments of Cr, Ni, and Si and depletion of Fe at temperatures from 376 °C to 524 °C and to a maximum dose of 35 dpa [27].

The capability to emulate neutron irradiation effects has been demonstrated by proton and heavy ion irradiation [29–33], which provide precisely controlled irradiation conditions for understanding changes to microstructure. Even so, a broad, systematic comparison of irradiation effects in promising commercial and advanced alloys has never been performed under identical conditions. The objective of this study is to provide a comprehensive microstructural characterization of several candidate materials for structural application in LWRs using proton irradiation identifying the most promising radiation tolerant materials. The irradiated microstructure will be discussed in terms of both composition effects and crystal structure.

#### 2. Experimental

Thirteen nickel-base and iron-base alloys were investigated in this study: eight nickel-base alloys (690, C22, 625, 625Plus, 625DA, 725, 718, and X750), three austenitic stainless steels (316 L, 310, and 800), and two ferritic alloys (T92 and 14YWT). Alloys 316 L and X750 served as control materials for low and high strength alloys, respectively. Alloys 690 and 625DA were supplied by Bechtel Marine Propulsion Corporation, alloys T92 and 14YWT were provided by Oak Ridge National Laboratory, alloy 316 L was provided by Crucible Industries, and all the other alloys were provided by Carpenter Technology Corporation. Heat numbers and chemical compositions are summarized in Table 1, and heat treatments are given in Table 2.

Many of the nickel-base alloys studied here are interrelated. For example, alloy 625 is available commercially in a variety of thermo-mechanical treatments. Alloy 625 is commonly used as a solid solution alloy, while an aged version is designated as 625Plus, and a hot-worked, direct aged (high-strength) version is referred to as 625DA. Similarly, alloy 725 is fabricated by increasing the Ti content of alloy 625 by a factor of five, giving a faster aging response [34]. Alloy 600 serves as the basis for alloys X750 and 690, which are modified by precipitation-hardening, and increased Cr content (for improved corrosion resistance), respectively. Alloy 718 is optimized from various thermomechanical treatments described in Refs. [35,36]. Among the alloys studied here, 625, 690, C22, 316 L, 310, 800, and T92 are considered as low strength alloys. Alloys 625Plus, 625DA, 725, 718, X750, and 14YWT, in contrast, were either precipitation hardened or disperse-strengthened and are therefore targeted for high strength applications. Among the precipitation hardened nickel-base alloys, alloy X750 is hardened by the L12-ordered Ni<sub>3</sub>(Al, Ti) ( $\gamma'$ ) phase, while alloys 625D, 625 P, and 725 derive their strength from D0<sub>22</sub>-ordered Ni<sub>3</sub>(Nb, Ti) ( $\gamma''$ ) phase. Only alloy 718 is hardened by both  $\gamma'$  and  $\gamma''$  precipitates.

Square bars,  $2 \times 2 \times 20$  mm, were cut from the as-received (AR) billets. The samples were polished with SiC down to 800 grit, and then electropolished to remove any deformed layer. Electropolishing was performed for 30 s at -30 °C and 20–40 V, using methanol solutions containing either 20 vol% sulfuric acid in the case of several nickel-base alloys, or 10 vol% perchloric acid for the others.

Irradiations with 2 MeV protons (one alloy per irradiation) were conducted using a 3 MV National Electronics Corporation Pelletron accelerator in the Michigan Ion Beam Laboratory (MIBL) at the University of Michigan. Irradiations were performed at a temperature of 360 °C and a chamber vacuum pressure below  $1 \times 10^{-7}$  torr. This experimental temperature was selected using

Download English Version:

# https://daneshyari.com/en/article/11006991

Download Persian Version:

https://daneshyari.com/article/11006991

Daneshyari.com